Transport in Porous Media **43:** 87–105, 2001.

A Two-Dimensional Areal Model for Density Dependent Flow Regime

S. SOREK[1,2], V. S. BORISOV[1] and A. YAKIREVICH[1]
[1] *J. Blaustein Institute for Desert Research, Environmental Hydrology & Microbiology, Ben-Gurion University of the Negev, Sede Boker Campus, 84990, Israel*
[2] *Mechanical Engineering, Pearlstone Center for Aeronautical Studies, Beer Sheva, 84105, Israel*

Abstract. A two-dimensional (2D) plane model of saltwater intrusion was developed, for the simulation of groundwater level and the average solute concentration in a 2D horizontal plane, together with the estimation of the saltwater depth. The proposed approach is of particular interest when assessing the effect of different regional pumping scenarios on groundwater level and its quality. The corresponding MEL2DSLT code was developed on the basis of the Modified Eulerian–Lagrangian (MEL) method to overcome difficulties arising from hyperbolic behavior of flow and transport equations, due to the advective nature of solute transport and heterogeneity of the soil characteristics (permeabilities and dispersivities). The code was verified against the 2D cross sectional model SUTRA and the three-dimensional (3D) model SWICHA. Simulation was conducted concerning the problem of saltwater intrusion in the Khan Yunis portion of the phreatic coastal aquifer of Gaza Strip. After calibrating the model for the aquifer parameters, we investigated its predictions resulting from various regional pumping scenarios using the actual pumping intensity from the year 1985 and extrapolating on the basis of 3.8% annual population growth. Results show a considerable depletion of groundwater level and intrusion of seawater due to excessive pumping.

Key words: coastal aquifer, seawater intrusion, averaging, 2D horizontal plane mathematical model.

1. Introduction

During last decades numerous models have been elaborated to simulate density dependent water flow and solute transport in porous media. These concern sharp-interface models (e.g. Bear and Dagan, 1964; Bear, 1972; Bear and Verruijt, 1987) and miscible advective–dispersive solute transport models (see survey by Sorek and Pinder, 1999).

Simulations of seawater intrusion into coastal aquifers based on the sharp-interface model follow the Badon Ghyben-Herzberg idealization, i.e, the flow is assumed to be that of no mixing salt water and fresh one, static equilibrium and a hydrostatic pressure distribution. Cooper's (1959) observations indicate that under certain conditions the width of the transition zone between fresh and salt water can be very wide to the extent that the sharp-interface model is no longer valid.

Cross-sectional advective–dispersive transport models (e.g., Voss, 1984; Sanford and Konikow, 1985) avoid complicated and expensive three-dimensional (3D) numerical simulations. However, such models do not allow simulating the effect of different pumping/recharge scenarios distributed over the horizontal plane. The 3D models (e.g. Huyakorn *et al.*, 1987; Sauter *et al.*, 1993; Diersch, 1988; Gambolati *et al.*, 1999) allow the most rigorous formulation of the saltwater intrusion problems. However, some difficulties can be encountered when dealing with simulation of large-scale aquifers. These are, for example: the data availability to perform model calibration; the numerical problems associated with the oscillations and numerical dispersion when solving advective–dispersive equation; the excessive computer time consumption arising from large number of grid nodes or blocks.

To simplify the solution, Strack (1995) developed a model for 3D variable-density flow, which in fact is based on hydrostatic pressure distribution. The problem is posed in terms of a discharge potential for single-density flow (Maas and Emke, 1988). This allows model formulation as a system of two-dimensional (2D) flow and 3D transport equations. This approach was implemented to a confined aquifer with horizontal upper and lower boundaries.

Our objective was to develop a 2D horizontal plane advective–dispersive model for a phreatic aquifer to address regional groundwater management in case of salt dependent flow regime and to overcome inherent difficulties associated with the application 3D models. To develop such a model we averaged the 3D flow and transport equations, along the vertical direction, over the saturated zone, without referring to the Dupuit assumption as well as to the one by Ghiben-Herzberg. The numerical algorithm is briefly described and some additional parameters appearing in the model as a result of the averaging procedure are discussed. The developed MEL2DSLT code was verified in compare to results obtained by a 2D cross-sectional code SUTRA (Voss, 1984) and a fully 3D code SWICHA (Huyakorn *et al.*, 1987). The model was applied to simulate seawater intrusion in the Khan Yunis portion of the coastal aquifer of Gaza Strip.

2. Averaging of the 3D Flow and Transport Equations

Figure 1 depicts a schematic view of the modeled hydrogeological system concerning saltwater intrusion into coastal aquifer. The following assumptions constitute the conceptual model. (1) Water flow is limited to the phreatic aquifer. (2) The water carries a non-volatile contaminant that can be adsorbed on the solid as well as decayed. The adsorption is governed by a linear equilibrium isotherm. (3) The dispersive and diffusive fluxes of the liquid are much smaller than the advective one. (4) Porosity is assumed to be dependent on pressure. (5) Density and viscosity of the liquid are assumed to be dependent on the solute concentration. Solid's density remains practically constant. (6) Solid's velocity is much smaller than that of liquid.

The Eulerian form of the water flow and solute transport equations are given in the form (Bear and Verruijt, 1987):

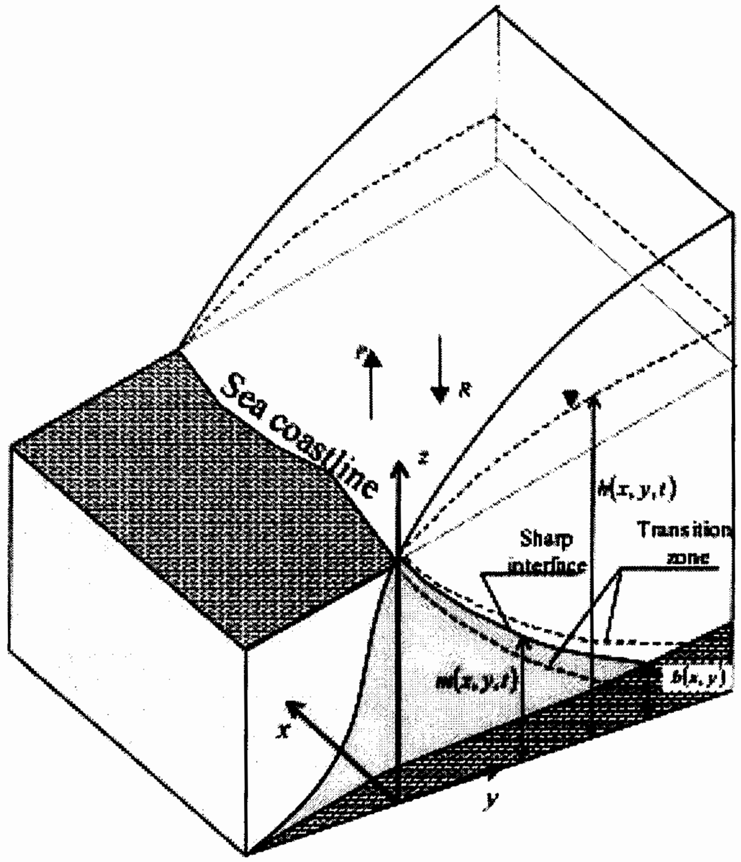

Figure 1. Idealization of the modeled subsurface system.

The liquid mass balance equations

$$\frac{\partial(\phi\rho)}{\partial t} + \nabla \cdot (\phi\rho\mathbf{V}) = \rho_R Q_R - \rho Q_P \tag{1}$$

where $\mathbf{V}$ denotes velocity of the liquid, $\phi(p)$ denotes the pressure (p) dependent porosity, $\rho(c)$ denotes the liquid density being a function of mass solute concentration (c), ρ_R denotes the density of a liquid recharged with a rate Q_R, and Q_P denotes the pumping rate.

The liquid linear (Darcy) momentum balance equation,

$$\phi\mathbf{V} = -\frac{\mathbf{k}}{\mu} \cdot (\nabla p - \rho\,\mathbf{g}) = -\mathbf{K} \cdot \left(\nabla H + \frac{\rho - \rho_0}{\rho_0}\nabla_z\right) \tag{2}$$

where $\mathbf{k}$ denotes the intrinsic permeability tensor, $\mathbf{g}$ denotes the vector of gravitational acceleration, $\mu(c)$ denotes the liquid viscosity, $\mathbf{K} = (\mathbf{k}g\rho_0/\mu)$ denotes the hydraulic conductivity, z denotes elevation parallel to $\mathbf{g}$, and $H = \Psi + z$, ($\Psi \equiv$

$p/g\rho_0$) denotes the hydraulic head with reference to ρ_0, which denotes the density of fresh liquid, and Ψ denotes the fresh liquid pressure head.

The solute mass balance equation for the porous medium,

$$\frac{\partial}{\partial t}[\phi\rho c R_d] = \nabla \cdot [\phi\rho(c\mathbf{V} - \mathbf{D}_c \cdot \nabla_c)] - \eta\phi\rho c R_d + c_R \rho_R Q_R - c\rho Q_p \tag{3}$$

in which $\mathbf{D}_c$ denotes the hydrodynamic dispersion tensor, $R_d = 1 + \rho_{\text{sm}} k_d (1 - \phi)/\phi$ denotes the retardation factor, ρ_{sm} denotes the solid matrix density, k_d denotes the partitioning coefficient, η denotes the rate decay coefficient, and c_R denotes the concentration of the solute associated with the injected liquid, and constitutive relations are given in the form,

$$\chi_c^\rho \equiv \frac{1}{\rho}\frac{\partial \rho}{\partial c}, \qquad \chi_P^\phi \equiv \frac{1}{1-\phi}\frac{\partial \phi}{\partial P}. \tag{4}$$

Bearing in mind that the vertical component of the fluid is usually small, we will consider two almost opposite premises. The first, when assuming that the vertical pressure is hydrostatic and thus the vertical velocity is zero. The second, by referring to a sharp interface model (Bear, 1972) for which the vertical velocity is not vanishing.

Consider a phreatic aquifer (Figure 1) and let $h(x, y, t)$ and $b(x, y)$ denote the upper (i.e. at the point where $p = 0$) and lower elevations, respectively, and $(\ )_h$, $(\ )_b$ denote values at the elevations h and b, respectively. The vertical averaged, $\overline{(\cdots)}$, flow and transport equations in a 2D horizontal plan, can be obtained by integrating ($\equiv 1/(h - b) \int_b^h (\cdots) \mathrm{d}z$) all terms in (1) to (3) by applying Lebnitz rule. In the process of averaging, we assumed that:

(1) The average over a product is approximately equal to the product of the averaged terms. In doing so we estimated the residual, verifying if it was much less in compare to the product of the averaged terms. In the case of the averaged dispersive flux, we accepted the notion that $\overline{\mathbf{D}_c \cdot \nabla' c} \approx \overline{\mathbf{D}_c} \cdot \overline{\nabla' c}$, following developments concerning 2D plane models (Bear, 1972 and Bear and Verruijt, 1987);

(2) The product of velocities with their spatial derivatives are negligible (Polubarinova-Kochina, 1977). Following Bear and Verruijt (1987), we write the balance equations at the upper and lower elevations of the phreatic aquifer, respectively, in the form

$$S_y \frac{\partial (z - h)}{\partial t} + [(\phi\mathbf{V})_h - \mathbf{q}_h] \cdot \nabla (z - h) = 0, \tag{5}$$

$$[(\phi\mathbf{V})_b - \mathbf{q}_b] \cdot \nabla (z - b) = 0, \tag{6}$$

where S_y denotes the specific yield. We assume that liquid fluxes are essentially vertical above the phreatic surface and below the aquifer bottom, i.e., $\mathbf{q}_h =$

$\{0, 0 - q_h\}$ and $\mathbf{q}_b = \{0, 0, q_b\}$. Therefore (5) and (6) can be rewritten in the form

$$(\rho\phi\mathbf{V})_h \cdot \nabla(z-h) = \rho_h S_y \frac{\partial h}{\partial t} - \rho_h q_h, \tag{7}$$

$$(\rho\phi\mathbf{V})_b \cdot \nabla(z-h) = \rho_b q_b. \tag{8}$$

Following Borisov and Manukian, (1985) and Yakirevich *et al.* (1998) and taking into account that the normal fluxes at both sides of the phreatic surface are equal, i.e., $(\rho\phi\mathbf{V})_{z=h+0} = (\rho\phi\mathbf{V})_h \cdot \nabla(z-h)$, we write

$$(\rho\phi\mathbf{V})_{z=h+0} = \rho_h S_y \frac{\partial h}{\partial t} - \rho_h q_h. \tag{9}$$

Similarly, writing the mass balance equation for solute at the upper and lower elevations of the phreatic aquifer, we obtain respectively

$$(c\phi\mathbf{V} - \phi\mathbf{D}_c \cdot \nabla c)_h \cdot \nabla(z-h) = c_h S_y \frac{\partial h}{\partial t} - c_h q_h, \tag{10}$$

$$(c\phi\mathbf{V} - \phi\mathbf{D}_c \cdot \nabla c)_b \cdot \nabla(z-b) = c_b q_b. \tag{11}$$

Averaging of (1) to (3) along the vertical and accounting for (4) and (7) to (11), yields the 2D horizontal plane equation of flow in the form

$$\begin{aligned}\alpha_{11}\frac{\partial h}{\partial t} + \alpha_{12}\frac{\partial \overline{c}}{\partial t} &= \nabla' \cdot \left[(h-b)\overline{\rho}\overline{\mathbf{K}}\left(\overline{\rho}\nabla' h + \frac{h-b}{2}\frac{\nabla'\overline{\rho}}{\overline{\rho}}\right)\right] + \\ &\quad + \rho_h q_h + \rho_b q_b + (h-b)(\overline{\rho_R Q_R} - \overline{\rho Q_P}),\end{aligned} \tag{12}$$

the specific discharge ($\mathbf{u}$) in the case of the hydrostatic pressure distribution is given by

$$\mathbf{u} = -\overline{\mathbf{K}}\left[\nabla' h + 0.5(h-b)\frac{\nabla'\overline{\rho}}{\overline{\rho}}\right], \tag{13}$$

and the transport equation

$$\begin{aligned}&\alpha_{21}\frac{\partial h}{\partial t} + \alpha_{22}\frac{\partial \overline{c}}{\partial t} - \nabla'(h-b)\overline{\rho}(\overline{c\phi\mathbf{V}} - \overline{\mathbf{D}}_c \cdot \overline{\nabla' c}) + \rho_h c_h q_h + \\ &\quad + \rho_b c_b q_b + \overline{R_d}(h-b)\eta\overline{\phi}_0\overline{\rho c} + (h-b)(\overline{\rho_R c_R Q_R} - \overline{\rho c Q_P}),\end{aligned} \tag{14}$$

where

$$\begin{aligned}\alpha_{11} &= \rho_h S_y + \overline{\rho}^2 g(1-\overline{\phi}_0)\chi_p^{\phi}(h-b) + \overline{\phi}_0(\overline{\rho} - \rho_h), \alpha_{12} = \overline{\phi}_0\overline{\rho}\chi_c^{\rho}(h-b), \\ \alpha_{21} &= \rho_h c_h S_y + \overline{\rho}^2 g\overline{c}(1-\overline{\phi}_0)\chi_p^{\phi}(h-b)\overline{R}_d + \\ &\quad + \overline{\phi}_0[\overline{\rho}(\overline{c} - c_h) + \overline{c}(\overline{\rho} - \rho_h)\overline{R_d}], \\ \alpha_{22} &= \overline{\rho}\overline{\phi}_0(h-b)(1 + \overline{c}\chi_c^{\rho})\overline{R_d},\end{aligned}$$

$\overline{\phi}_0$ denotes the averaged porosity at the reference pressure.

Expression (13) can be considered as a good approximation in regions where the vertical flow component is indeed small. However, following Bear (1972) and Segol (1994) for saltwater intrusion problems, this assumption is not always justified for flow in the transition zone between the fresh and saline water. Let us, therefore, obtain an estimation of the specific discharge by using the sharp interface model which accounts separately for the saltwater, $(\;)_s$, and the freshwater, $(\;)_F$, zones and does not assume hydrostatic pressure distribution in the aquifer. We assume that $\mathbf{K}_s \approx \mathbf{K}_F$ with a maximum error of about 4% (Sorek *et al.*, 1999),* and we write the fluid mass balance equation with relation to m, the sharp interface elevation (Figure 1), and $\overline{\rho}$ that is associated with the 2D plane model,

$$\rho_s(m-b) + \rho_F(h-m) = \overline{\rho}(h-b) \tag{15}$$

from which, we deduce that

$$m = \omega h + (1-\omega)b, \qquad \omega = \frac{\overline{\rho} - \rho_F}{\rho_S - \rho_F}. \tag{16}$$

In view of (15), we can in a similar way obtain, $\overline{\mathbf{u}}$, the averaged specific discharge in relation to the sharp interface model. We thus write

$$\overline{\mathbf{u}}(h-b) = \mathbf{u}_S(m-b) + \mathbf{u}_F(h-m),$$

or

$$\overline{\mathbf{u}} = \omega \mathbf{u}_S + (1-\omega)\mathbf{u}_F. \tag{17}$$

We evaluate $\mathbf{u}_F$ and $\mathbf{u}_S$ in the fresh and salt zones, respectively,

$$\mathbf{u}_F = -\overline{\mathbf{K}} \cdot \nabla' h, \tag{18}$$

$$\mathbf{u}_S = -\overline{\mathbf{K}} \left[\nabla' h + (h-b)\nabla' \frac{\overline{\rho}}{\rho_s} - \frac{\rho_s - \overline{\rho}}{\rho_s} \nabla'(h-b) \right]. \tag{19}$$

After substituting (18) and (19) into (17) we obtain

$$\overline{\mathbf{u}} = -\overline{\mathbf{K}} \cdot \left[\nabla' h + \omega(h-b)\nabla' \frac{\overline{\rho}}{\rho_s} - \frac{(\overline{\rho} - \rho_F)(\rho_s - \overline{\rho})}{(\rho_s - \rho_F)\rho_s} \nabla'(h-b) \right]. \tag{20}$$

It can be shown that the coefficient of $\nabla'(h-b)$ is much smaller than a unit (the coefficient of $\nabla' h$), i.e.

$$\max_{\overline{\rho}} \frac{(\overline{\rho} - \rho_F)(\rho_s - \overline{\rho})}{(\rho_s - \rho_F)\rho_s} = 0.25 \frac{\rho_s - \rho_F}{\rho_s} \approx 6 \times 10^{-3} \ll 1, \quad \text{for } \rho_s = 1.025\rho_F,$$

therefore the last term in (20) is negligible. Hence we rewrite (20) to read

$$\overline{\mathbf{u}} = -\overline{\mathbf{K}} \cdot \left[\nabla' h + \omega(h-b)\nabla' \left(\frac{\overline{\rho}}{\rho_s} \right) \right]. \tag{21}$$

* Note that the resultant vertical averaged conductivity on the basis of the $\mathbf{K}_S$ and $\mathbf{K}_F$ values has an error of 2% maximum.

The principle difference between (13) and (21) is in the coefficients of the second terms in the right-hand sides of these equations. Realizing that (13) and (21) are two realizations based on almost two opposite premises, we postulate that the averaged specific discharge can be evaluated by

$$\mathbf{u} = -\overline{\mathbf{K}} \cdot \left[\nabla' h + \Omega (h-b) \frac{\nabla' \overline{\rho}}{\rho_s} \right], \tag{22}$$

where the dimensionless parameter Ω is a function of the density $\overline{\rho}$. We note that (22) can be regarded as the generalization of Dupuit assumption for density dependent flow.

For the averaged transport Equation (14) we need to account for the variations of the horizontal velocities along the vertical direction. We note that for $\overline{c\phi\mathbf{V}}$ we cannot follow the notion of being approximately equal to $\overline{c}\overline{\phi\mathbf{V}}$ due to strong variations (and change of flow direction) along the vertical direction of the specific flux. Hence, to estimate, $\overline{c\phi\mathbf{V}}$, the average advective term we, analogously to (15), refer to a sharp interface model. We thus write .

$$(h-b)\,\overline{c\phi\mathbf{V}} = \mathbf{u}_s \int_b^m c\,\mathrm{d}\zeta + \mathbf{u}_F \int_m^h c\,\mathrm{d}\zeta. \tag{23}$$

We obtain following expression

$$\overline{c\phi\mathbf{V}} = \mathbf{u}\overline{c} - \xi\overline{c}(1-\Omega)(h-b)\overline{\mathbf{K}} - \cdot\nabla' \frac{\overline{\rho}}{\rho_s} \tag{24}$$

where

$$\xi \approx 1 - \frac{1}{\overline{c}(h-m)} \int_m^h c\,\mathrm{d}z. \tag{25}$$

Taking into account (4), (22) and (24), the Eulerian form of the balance equations to simulate saltwater intrusion for a 2D horizontal plane become:
The flow equation

$$\begin{aligned} \alpha_{11}\frac{\partial h}{\partial t} + \alpha_{12}\frac{\partial \overline{c}}{\partial t} &= \nabla' \cdot \{(h-b)\overline{\rho}\overline{\mathbf{K}} \cdot [\nabla' h + \Omega(h-b)\chi_c^{\rho}\nabla'\overline{c}]\} + \\ &\quad + \rho_h q_h + \rho_b q_b + (h-b)(\overline{\rho_R Q_R} - \overline{\rho Q_p}). \end{aligned} \tag{26}$$

The specific discharge

$$\mathbf{u} = -\overline{\mathbf{K}} \cdot [\nabla' h + \Omega(h-b)\chi_c^{\rho}\nabla'\overline{c}]. \tag{27}$$

The transport equation

$$\begin{aligned} \alpha_{21}\frac{\partial h}{\partial t} + \alpha_{22}\frac{\partial \overline{c}}{\partial t} &= -\nabla' \cdot [(h-b)(\mathbf{u}\overline{c} - \mathbf{D}\cdot\nabla'\overline{c})] + \rho_h c_h q_h + \rho_b c_b q_b + \\ &\quad + \overline{R_d}(h-b)\eta\overline{\phi}_0\overline{\rho c} + (h-b)(\overline{\rho_R c_R Q_R} - \overline{\rho c Q_P}), \end{aligned} \tag{28}$$

where

$$\mathbf{D} = \phi\overline{\mathbf{D}}_c + \xi(1-\Omega)\bar{c}(h-b)\chi_c^{\rho}\overline{\mathbf{K}}, \tag{29}$$

in which $\overline{\mathbf{D}}_c$ denotes the vertically averaged hydrodynamic dispersion tensor.

Based on physical considerations, series of simulations and comparison with results obtained with the hydrodynamic advective–dispersive models SUTRA and SWICHA, the $\Omega = \Omega(\overline{\rho})$ parameter was approximated in the form

$$\Omega = \Omega_0\left(\frac{\overline{\rho}-\tilde{\rho}}{\rho_s-\tilde{\rho}}\right)^{v} \tag{30}$$

where ρ_s denotes the sea water density, $\tilde{\rho} = 0.958$ kg/kg which matches the density of boiling fresh water at natural conditions (i.e. temperature 20°C, pressure 1 atm.), v and Ω_0 are dimensionless fitting parameters. We note that on the basis of the two limiting cases (hydrostatic regime and the sharp interface approach) the limits associated with Ω_0 become $0.5 \leqslant \Omega_0 \leqslant 1$.

The factor ξ in (29) is associated with additional dispersion due to variations in the fluid horizontal velocities along the vertical direction. It was evaluated on the basis of (25) so as to be equal to a unit for the case of a sharp interface and less than a unit when accounting for dispersion. As we assume that dispersion is not explicitly affected by the variability of the liquid density, we evaluated the second term of (25) using the analytical solution of Cleary and Ungs (1978) of 2D advection–dispersion equation with constant velocity and fluid density. The formulation of the factor ξ reads

$$\xi = \frac{a_A}{a_A + \sqrt{a_L a_T}} \tag{31}$$

where a_L and a_T denote the longitudinal and transversal dispersivities, respectively, a_A denotes an additional apparent dispersivity.

Generally speaking, in field studies we do not measure parameters directly (e.g. hydraulic conductivities and dispersivities) that are artifact of our modeling concepts. Moreover, in the process of calibration (in itself, non-unique inherently) we many times change those 'measured' values so as to fit observations (or even observations at prescribed zones). Hence, the notion of the additional, Ω_0, v and a_A, parameters actually falls under the same considerations as the ones habitually used thus far for flow and transport models. Further more, it may be suggested that in the process of calibration, one can fix the parameters that we are accustomed to use and change only the additional ones to accommodate model predictions with field observations. Like other parameters the rule of the additional ones should also be verified by a sensitivity analysis as well as to asses their physical significance when comparing with measurements. This, although important in its own right, is beyond the scope of the manuscript.

The above flow, (26), specific flux, (27) and transport, (28), equations describe a complete model to simulate the saltwater intrusion problem in horizontal 2D configurations. These were transformed to the modified Eulerian–Lagrangian (MEL) form (Bear *et al.*, 1997; Sorek *et al.*, 1999) to overcome difficulties (numerical dispersion and spurious oscillations) arising from the hyperbolic behavior due to advective nature of transport and heterogeneity of the soil characteristics (permeability and dispersivity). A mathematical analysis (Sorek *et al.*, 2000) proves that for coupled partial differential equations, unlike the Eulerian finite difference scheme, the MEL method unconditionally guarantees the absent of spurious oscillation. A numerical example (Sorek *et al.*, 1999; Sorek *et al.*, 2000) suggests that the MEL scheme produces better resolution compared to the Eulerian and the Eulerian–Lagrangian ones. The developed MEL2DSLT code, which is based on the MEL formulation, implements a fully explicit scheme using the finite difference method.

3. Model Verification

We compared the MEL2DSLT code for 2D horizontal plan of a coastal phreatic aquifer, with the SUTRA code (Voss, 1984) which simulates the saltwater intrusion problem for an unsaturated/saturated cross section (i.e. averaged along the coastal line direction). To overcome these differences we imposed conditions that generated a 1D (horizontal, inland direction) flow and transport. The following aquifer properties were assigned: elevation of the aquifer bottom $b = -80$ m, hydraulic conductivity $K = 1$ m/day, specific yield $S_y = 0.3$, longitudinal and transversal dispersivities $a_L = 10$ and $a_T = 1$ m, respectively. The initial conditions were $h(x, y, 0) = 0$ and $\overline{c}(x, y, 0) = 0$. Along the sea boundary, we chose $h(x, 0, t) = 0$ and $\overline{c}(x, y, 0)/c_s = 1$ ($c_s = 35.7$ g/kg denotes the solute concentration of seawater), while $\overline{c}(x, y, 0)/c_s = 0$. At the $y = 500$ m, boundary, we had prescribed two different water levels $h(x, 500, t) = 0.5$ and $h(x, 500, t) = 1.5$ m, for two different simulations. Impervious boundary conditions were assigned for flow and transport along $x = 0$ and $x = 200$ m. These flow conditions generate a 1D flow and transport problem. Simulations for a 50 year period were performed using constant spatial increments of $\Delta x = 100$ and $\Delta y = 25$ m.

To enable the comparison for a phreatic aquifer, we used the pressure distribution obtained by SUTRA, and found, h, the groundwater level at the elevation where $p \equiv 0$. We also averaged the concentrations obtained by SUTRA over the thickness of the saturated zone. Such an averaging generates a 1D (along the y-direction) solute distribution.

The groundwater level and the concentration, simulated by MEL2DSLT, were compared with those obtained by SUTRA. Parameters $\Omega_0 = 1$, $v = 3.8$ and $a_A = 2.9$ m (see (29) and (30), respectively) were chosen by trial-and-error to obtain agreement between the MEL2DSLT and the SUTRA simulations, for the case of $h(x, 500, t) = 0.5$ m. These parameters were then used to simulate the case from which $h(x, 500, t) = 1.5$ m. Figure 2(a) demonstrates the groundwater levels for both cases, simulated by the SUTRA and MEL2DSLT codes. The averaged concentration profiles produced by MEL2DSLT also prove to be in very small deviation from those obtained by SUTRA (Figure 2(b)).

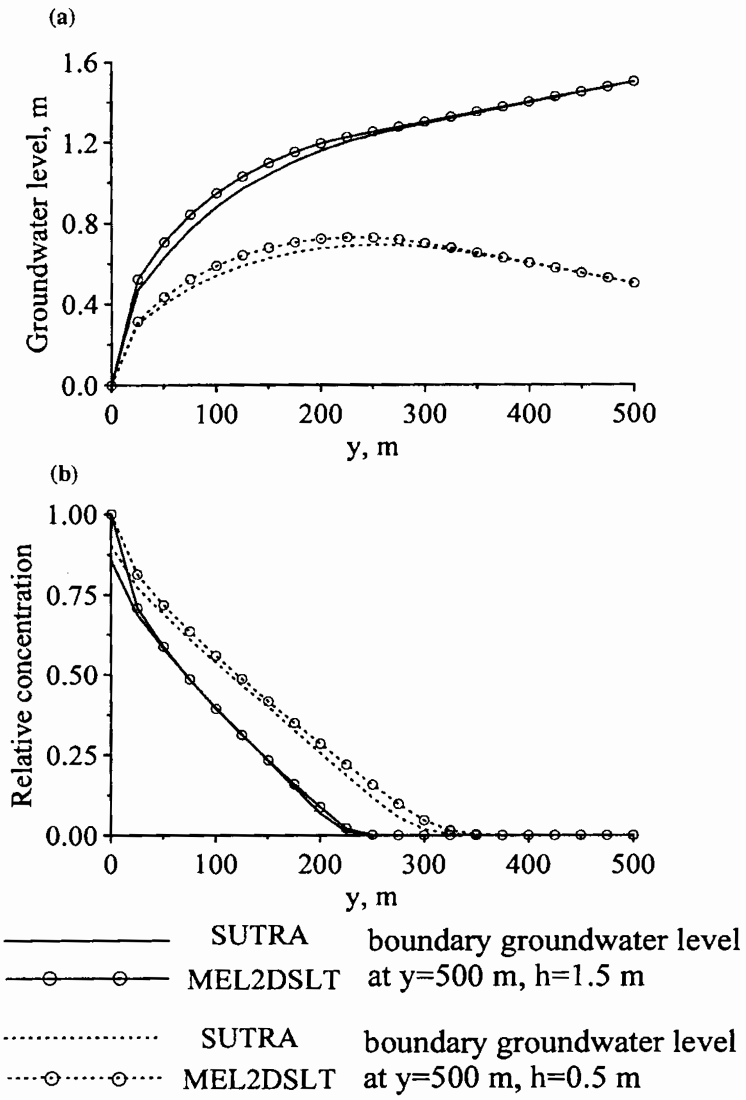

Figure 2. Comparison between simulations with SUTRA and with MEL2DSLT, after the time period of 50 years: (a) groundwater level; (b) distribution of concentration.

As demonstrated by the solution obtained with SUTRA (Figure 3), for a vertical cross section, a significant gradient of concentration is noticed. We note that the saltwater depth, estimated by (16), approximately follows the 0.5-isoconcentration line.

Numerical experiments comparing between the solutions obtained by SUTRA and MEL2DSLT proved that the extent of change of, a_A, the apparent dispersivity

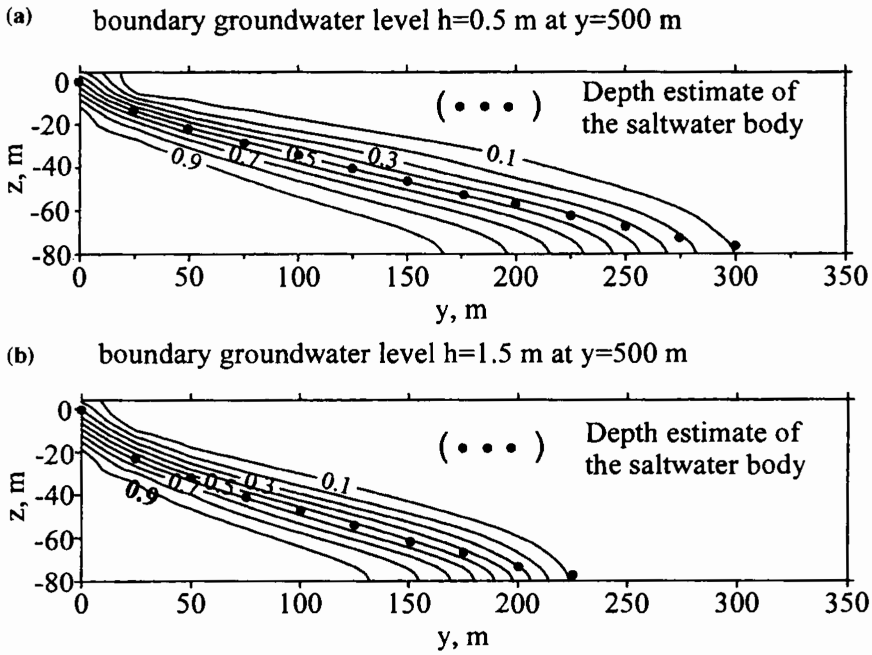

Figure 3. Concentration profiles obtained by SUTRA in a vertical cross section after 50 years and the MEL2DSLT estimate of the saltwater depth.

is significantly less than that of a_L and a_T, the longitudinal and transversal dispersivities, respectively. With $a_L = 25$ and $a_T = 2.5$ m (originally $a_L = 10$ m, $a_T = 1$ m and $a_A = 2.9$ m) we found that $a_A = 3$ m produced almost no deviation between the solution of SUTRA and that of MEL2DSLT (not shown).

The ability of the novel 2D horizontal plane model to simulate different regional pumping scenarios was demonstrated by the following example. We chose an overall area span between ($0 < x < 1000$ m) and ($0 < y < 1000$ m). The spatial increments were: $\Delta x = \Delta y = 50$ m. The period of pumping operation was 3650 days. Other parameters were chosen to be: $v = 3.8$; $S_y = 0.2$; $\alpha_A = 2.9m$; $\alpha_T = 0.1\alpha_L$. The area was composed of two distinct zones. The first zone $\{0 < x < 1000\,\text{m},\ 300 < y < 1000\,\text{m}\}$ was characterized by $\alpha_L = 5$ m and $K = 0.1$ m/day. Within this zone, the first pumping well is located at $\{x_1 = 0,\ y_1 = 600\,\text{m}\}$ with a flux of $Q_1 = 250\,\text{m}^3$/day. The second zone $\{0 < x < 1000\,\text{m},\ 0 < y < 300\,\text{m}\}$ was characterized by $\alpha_L = 10$ m and $K = 1$ m/day. Within the second zone another pumping well was situated at $\{x_2 = 500\,\text{m},\ y_2 = 200\,\text{m}\}$ with a flux of $Q_2 = 750\,\text{m}^3$/day. Along the $y = 1000$ m boundary, we assigned $c(x, y, t) = 0$ and $h(x, y, t) = 1$ m. Other conditions and parameters were taken from the previous example. Comparison (depicted in Figure 4) were made between the solutions obtained by MEL2DSLT and SWICHA (Huyakorn, 1987), which is

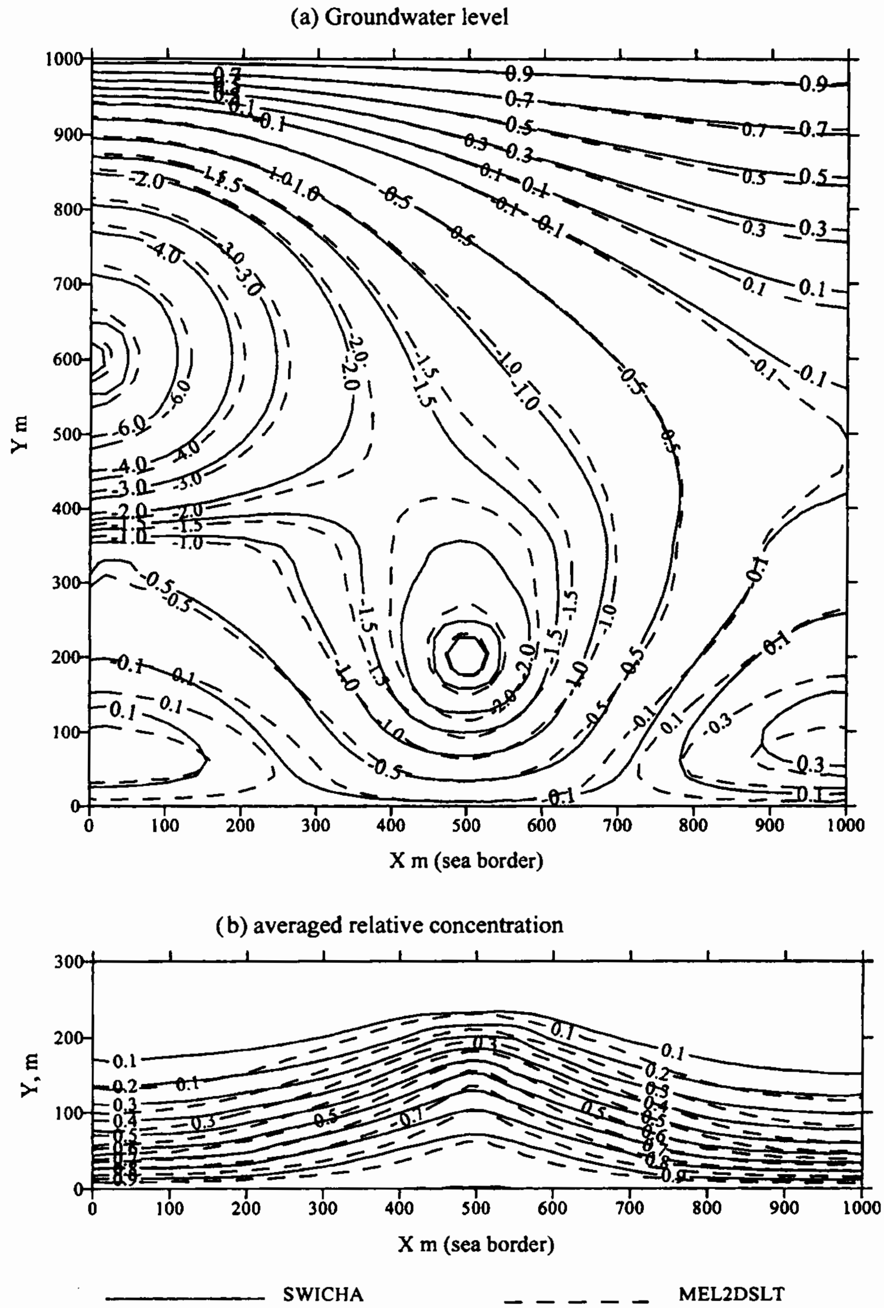

Figure 4. Comparison of simulation results after 10 years of pumping for the MEL2DSLT and SWICHA codes.

fully 3D density-dependent flow and transport model. To perform a comparison with the solution obtained by SWICHA, we referred to the groundwater level as the depth at which $p = 0$. We then used this spatial varying depth to average the 3D concentration values so that the outcome will be distribution along a 2D horizontal plane. We note that actually we used the same values of the parameters ($\Omega_0 = 1$, $\upsilon = 3.8$ and $\alpha_A = 2.9$ m) as in the previous comparison made with the SUTRA code. Yet, Figure 4 demonstrates consistent agreement between the MEL2DSLT code and the SWICHA code.

4. Application to the Gaza Strip Coastal Aquifer

We consider the seawater intrusion problem into the coastal aquifer of Gaza strip, focusing on the Khan Yunis region (Figure 5). The coastal aquifer of the Gaza Strip region is a Pleistocene-age granular aquifer. It extends from Ashqelon in the north to Rafah in the south, and from the seashore on the west to the Israeli settlements Erez, Kissufim, Nirim, and Nahal Oz on the east (Figure 5(a)). For management purposes, the aquifer of the Gaza strip is subdivided into four regions: Gaza, Nuseirat, Deir el Balah, and Khan Yunis/Rafah. Each of these regions is subdivided into cells, hydrologic strips, and columns (Figure 5(a)).

The coastal aquifer is composed of layers of dune sand, sandstone, calcareous sandstone, silt, with intercalations of clay and loam. Some of the layers are lenses; others begin at the coast and separate the aquifer into various subaquifers, designated as A, B1, B2, and C (Figure 5(b)). Subaquifer A is phreatic, whereas B1, B2, and C become confined towards the sea. The aquifer overlies marine clay of Neogene age, known as the Saqiye Clay aquiclude (Fink, 1970; Melloul and Bachmat, 1975). The aquifer bottom is not horizontal (Figure 5(b)) and total thickness of the saturated zone varies from 100 m at the sea border to 28 m, at the eastern boundary.

Actually, such a multi-aquifer system should be simulated by fully 3D model (as appears in the report by Metcalf and Eddy, 2000), however, such models require significantly more computing resources as well as field data. Hence, using 3D models for optimal management is restricted.

Had the physical parameters been, say, a prescribed function of the vertical direction then these would have been subject to the averaging procedure. However, in the case of a multi-aquifer system with parameters of many orders different across adjacent layers along the vertical direction, we need to tailor (using jump conditions and adjusting vertical fluxes at the common boundaries) the balance equations between two adjacent aquifers. Such a case is actually the flow and transport problems of the Gaza aquifer. We had circumvented these problems, for the Gaza aquifer, by assuming an equivalent one-aquifer layer for which its physical parameters were chosen so as to obtain a good agreement between observed and simulated values of the primary variables. Hence, when considering the 2D plane formulation, these aquifers are lumped into one aquifer. In the case of a multi-aquifer system, we address the possible steep gradients in fluid velocities

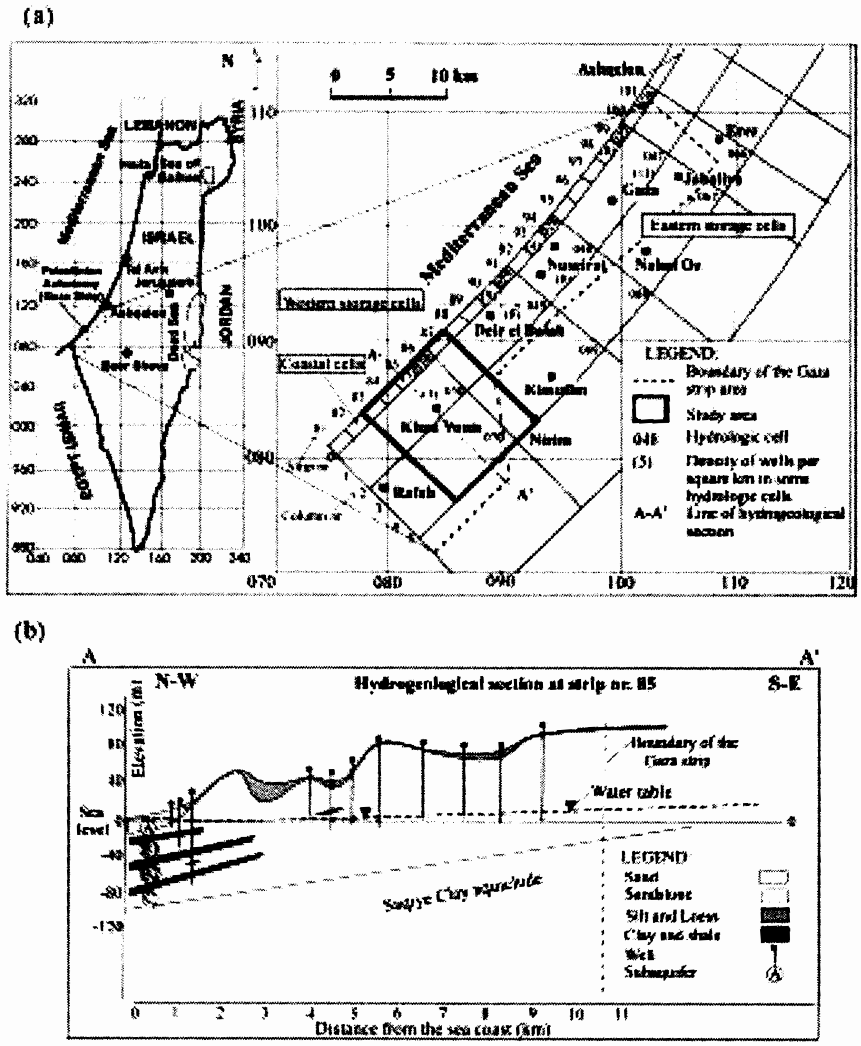

Figure 5. General view of (a) the Gaza strip, and (b) a typical hydro-geological cross section.

(and steep gradients of the aquifer parameters) by the MEL algorithm. With the current MEL2DSLT code, such steep gradients are accounted for only within a 2D horizontal plane. Actually, Figure 5(a) demonstrates characteristics for which we developed the MEL2DSLT code, i.e., to enable 2D horizontal plane assessment of different regional stress scenarios.

The amount of exploitation of the coastal aquifer in the entire Gaza region is based on data from approximately 2000 wells, with an average of 5 wells per km^2. In the Khan Yunis area, the density of wells is less than 4 wells per km^2. Depth of most of the pumping wells is 5–10 m below the groundwater level, namely the water is being pumped from within the phreatic aquifer.

The model was calibrated (Sorek *et al.*, 1999) using hydrogeological information within a region limited from North–West by the coastal line from strips 83 to 86 and stretching North-East 8 km inland. This area (8 × 8 km) was divided by rectangular cells 200 m × 200 m each, altogether 41 × 41 = 1681 nodes. Information regarding concentration values was scarce and not reliable. We therefore, calibrated the model using mainly measured groundwater levels. Such, exists for the years 1985–1991, as well as values of pumping and natural replenishment. These data were not provided for all wells and was not observed at the same time. We chose a time step of one month to account for the diversity of observations at different time. Altogether 12 (month) ×7 (year) = 84 files of information were completed, each represents the distribution of the groundwater levels in a particular month from the years 1985–1991. These can be considered as 'slices' of a random field of groundwater levels in 84 time points. We had eliminated an inherent spatial plane distribution of a linear time trend in the random distribution of the groundwater levels (e.g., due the anthropogenic effects prevailing in the study area). We then evaluated the spatial distributions of the mean of the initial groundwater levels and those of the chloride (Cl^-) concentrations, at the beginning of the year 1985. Dirichlet conditions for the hydraulic head and for the Cl^- concentration were assigned at the boundaries. These conditions were the evaluated mean values based on observation in time along the boundaries.

For the sake of obtaining the estimated groundwater levels, simulation was conducted with: specific yield $S_y = 0.3$, porosity $\phi = 0.35$, for the averaged specific discharge we used longitudinal dispersivity $a_L = 25$ m, transversal dispersivity $a_T = 0.5$ m, the apparent dispersivity of $a_A = 2.7$ m, $\Omega_0 = 1$ and $v = 3.8$. We also accounted for, $C_h = 110$ mg/kg, an observed regional average annual Cl^- concentration associated with the natural replenishment. The comparison between the observed groundwater level and concentration distribution values for 1985 and 1991 and the simulated ones is given by Sorek *et al.* (1999).

After calibrating for the aquifer parameters, we investigated the model predictions resulting from possible stress patterns. Initial distribution of groundwater levels and concentrations were estimated by steady state simulation without source/sink stresses. On the basis of the obtained initial conditions, we implemented the pumping scenario (Figure 6) based on the actual pumping intensity from the year 1985 which was extrapolated on the basis of 3.8% annual population growth. The stipulated pumping scenario was the regional stress that changed the distributions of the groundwater levels (Figure 7(a)) and the chloride concentrations (Figure 7(b)). In view of this result, we note that predicted for the year 2006 groundwater levels will be considerably depleted, which will induce further seawater intrusion into the coastal aquifer. By virtue of (9) we can also assess the depth of the fresh water body (Figure 8). This actually enables us to estimate the salt migration in a quasi 3D space.

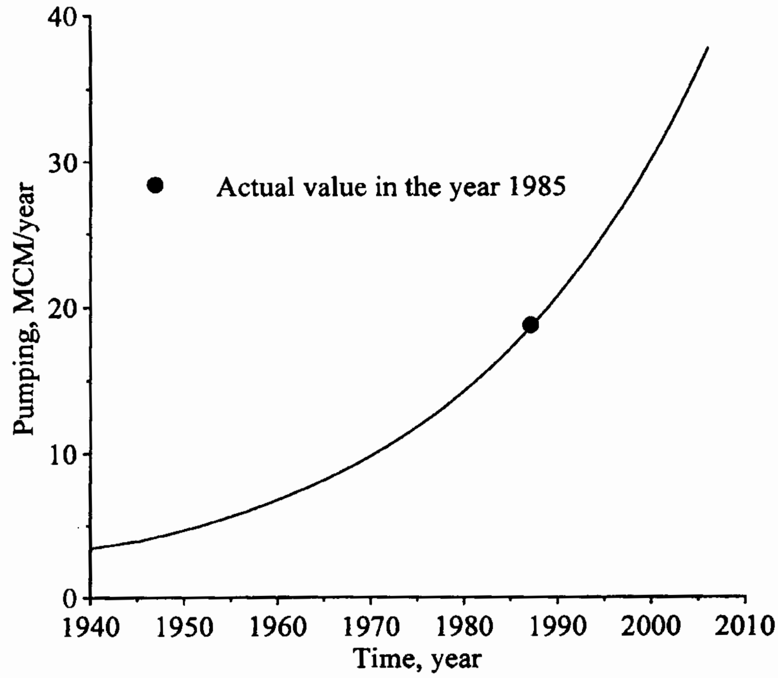

Figure 6. Scenario of the total pumping rate for the Khan Yunis region.

5. Summary

The governing equations were formulated to simulate the saltwater intrusion problem for 2D horizontal plane. The problem was solved numerically using an explicit finite difference method.

The Modified Eulerian–Lagrangian method was used to overcome the difficulties arising from the hyperbolic behavior of the flow and transport equations due to advective nature of transport and the heterogeneity of the soil characteristics (permeability and dispersivity). The resulting MEL2DSLT code was verified for a 1D case against a numerical solution obtained on the basis of the SUTRA code and a 2D case against the SWICHA code.

The MEL2DSLT code was implemented to simulate the seawater intrusion problem into the Khan Yunis section of the Gaza Strip Coastal aquifer, based on the actual pumping intensity from the year 1985 and extrapolating on the basis of 3.8% annual population growth. Results show a considerable depletion of groundwater level and intrusion of seawater due to excessive pumping. The developed approach is of particular interest to assess the effect of different regional pumping scenarios on groundwater level and its quality in coastal aquifers.

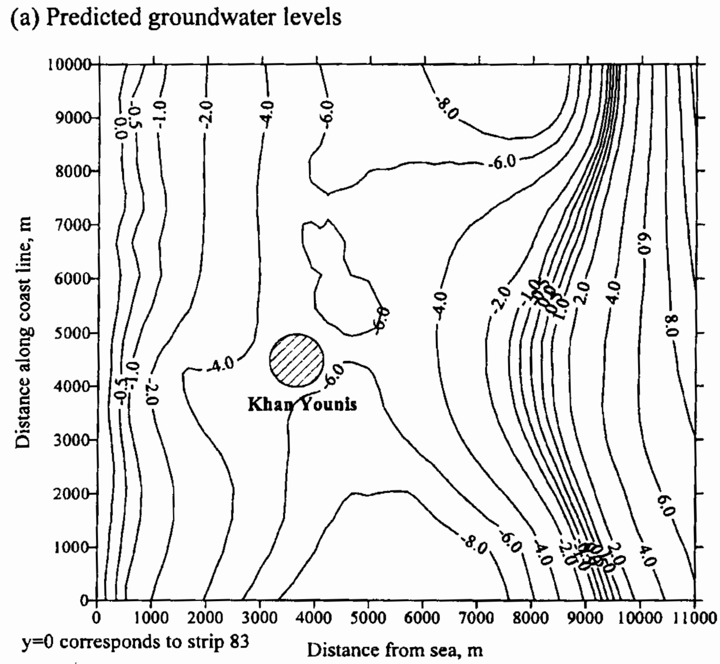

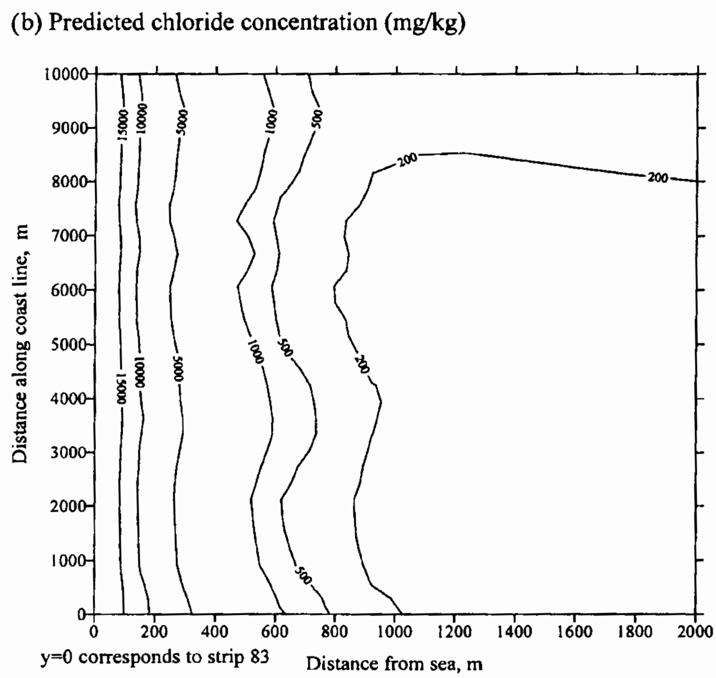

Figure 7. Simulation results for the Khan-Yunis portion of the Gaza coastal aquifer for the year 2006.

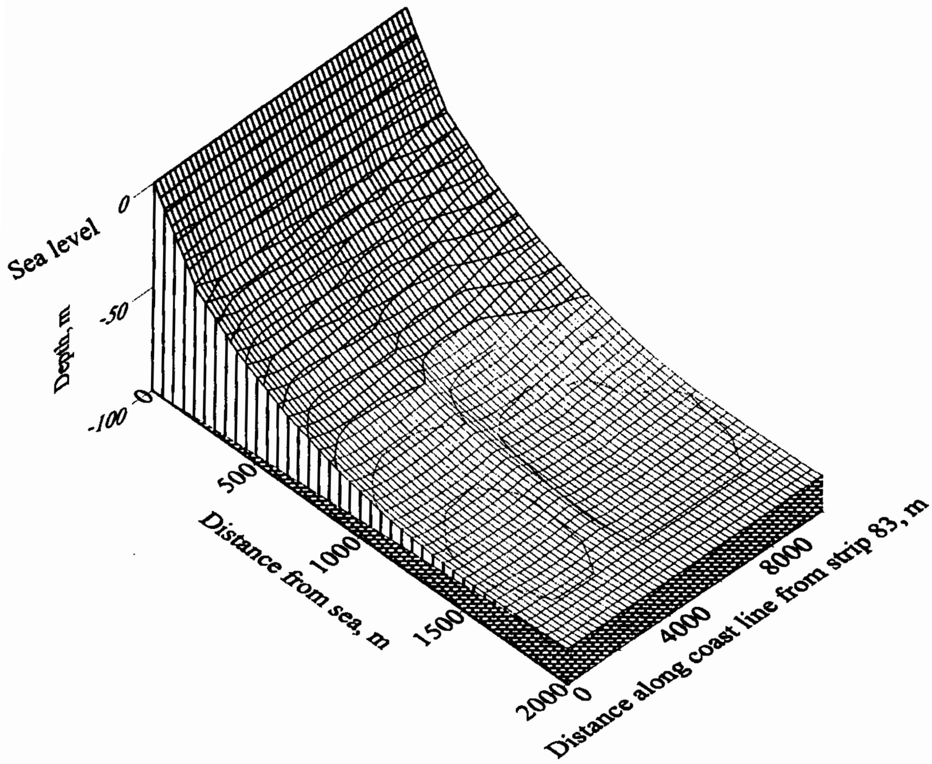

Figure 8. Estimate of the saltwater depth for year 2006.

References

Bear, J.: 1972, *Dynamics of Fluids in Porous Media*, Amer. Elsevier publishing Company, New York/London/Amsterdam.

Bear, J. and Dagan, G.: 1964, Moving interface in coastal aquifers, *ASCE J. Hydraulic Div.* **90**, 193–216.

Bear, J., and Verruijt, A.: 1987, *Modeling Groundwater Flow and Pollution*, D. Reidel Publish. Company, Dordrecht.

Bear, J., Sorek, S. and Borisov, V.: 1997, On the Eulerian–Lagrangian formulation of balance equations in porous media, *Numerical Methods for Partial Differential Equations* **13**, 505–530.

Borisov, V. S. and Manukian D. A.: 1985, Simulating of water and salt regime of soil when designing systems of irrigation, in: *Automatic preparation and management in water engineering*, VNIIGiM, Moscow, pp. 110–119 (in Russian).

Cleary, R. W., and M. J. Ungs: 1978, *Groundwater Pollution and Hydrology, Mathematical Models and Computer Programs*, Research Report No. 78-WR-15, Water Resour. Program, Prinston Univ. Prinston, New Jersey.

Cooper, H. H. Jr.: 1959, A hypothesis concerning the dynamic balance of fresh water and salt water in a coastal aquifer, *J. Geophys. Res.* **64**, 461–467.

Diersch, H. J.: 1988, Finite element modeling of recirculating density driven saltwater intrusion processes in groundwater, *Adv. Water Resour.* **11**, 25–43.

Fink, M.: 1970, The hydrogeology of the Gaza Strip. TAHAL report 3, Tel-Aviv [in Hebrew].

Gambolati, G., Putti, M., and Paniconi, C.: 1999, Three-dimensional model of coupled density-dependent flow and miscible salt transport in groundwater, In: J. Bear, A. H.-D. Cheng, S. Sorek, I. Herrera and D. Ouazar (eds), *Seawater Intrusion in Coastal Aquifers – Concepts, Methods and Practices*, Kluwer Academic Publishers, Dordrecht/Boston/London, pp. 315–362.

Huyakorn, P. S., Andersen, P. E., Mercer, J. W. and White, H. O., Jr.: 1987, Saltwater intrusion in aquifers: Development and testing of a three-dimensional finite element model, *Water Resour. Res.* **23**, 292–312.

Maas, C. and Emke, M. J.: 1988, Solving varying density groundwater problems with a single density computer program, *Natuurwet. Tijdschr.* **70**, 143–154.

Polubarinova-Kochina, P.Ya., *Theory of Groundwater Motion*, Nauka, Moscow, 1977 (in Russian).

Metcalf and Eddy, Inc.: 2000, Coastal aquifer management program: Final model report. Unpublished report under contract 294-C-00-99-00038-00 for U.S. Agency for International Development, Tel-Aviv.

Sanford, W. E. and Konikow, L. F.: 1985, *A Two-Constituent Solute Transport Model for Ground Water Having Variable Density*, USGS Water-Resources Investigations Report 85–4279.

Sauter, F. J., Leijnse, A. and Beusen, A. H. W.: 1993, METROPOL. User's guide. Report nr. 725205.003. National Institute of Public Health and Environment Protection. Bilthoven, The Netherlands.

Segol, G.: 1994, *Classic Groundwater Simulations: Proving and Improving Numerical Models*, PTR Prentice Hall, New Jersey.

Sorek, S., Borisov, V. and Yakirevich, A.: 1999, Modified Eulerian Lagrangian (MEL) method for density dependent miscible transport, In: J. Bear, A. H.-D. Cheng, S. Sorek, I. Herrera and D. Ouazar (eds), *Seawater Intrusion in Coastal Aquifers – Concepts, Methods and Practices*, Kluwer Academic Publishers, Dordrecht/Boston/London, pp. 383–398.

Sorek, S. and Pinder, G. F.: 1999,Survey of computer codes and case histories, In: J. Bear, A. H.-D. Cheng, S. Sorek, I. Herrera and D. Ouazar (eds), *Seawater Intrusion in Coastal Aquifers – Concepts, Methods and Practices*, Kluwer Academic Publishers, Dordrecht/Boston/London, pp. 383–398.

Sorek, S., Borisov, V., and Yakirevich, A.: 2000, Numerical modeling of coupled hydrological phenomena using the Modified Eulerian-Lagrangian Method. *The GSA Special Papers in honor of S. Neuman 60th birthday*, Paper 348, pp.151–160 (in Press).

Strack, O. D. L.: 1995, A Dupuit-Forchheimer model for three-dimensional flow with variable density, *Water Resour. Res.* **31**, 3007–3017.

Voss, C. I.: 1984, *SUTRA, a Finite-Element Simulation Model for Saturated–Unsaturated, Fluid-Density-Dependent Ground-Water Flow with Energy Transport or Chemically-Reactive Single Species Solute Transport*, Water Resources Investigations Report 84–4369, US Geological Survey.

Yakirevich A., Borisov, V. and Sorek, S.: 1998, A quasi three-dimensional model for flow and solute transport in unsaturated and saturated zones: I. Implementation of the quasi two-dimensional case, *Adv. Water Resour.* **21**, 679–689.